Journal of Agricultural Science and Technology (JAST), 29(2)
In Press, Pre-Proof Version

Assessing rain-fed cropland suitability under SSP scenarios: a case study of Qazvin Province, Iran

Mansoureh Kouhi[1]*, and Ebrahim Asadi Oskouei[1]

Abstract

Rain-fed agricultural productivity is increasingly threatened by rising temperatures and shifting precipitation patterns. This study evaluates the current and future suitability of rain-fed cropland in Qazvin Province, Iran—a region where such an assessment has not been previously conducted. Although Qazvin Plain comprises only 1% of Iran's land area, it contributes approximately 4% of national agricultural production. The study employs the Maximum Entropy (MaxEnt) model, integrating topographic and climatic factors to identify determinants of rain-fed cropland suitability. Suitability was assessed under optimistic (SSP1-2.6) and pessimistic (SSP5-8.5) scenarios using historical data (1985–2014) and future projections (2021–2040) from three CMIP6 models (MPI-ESM1-2, ACCESS-ESM1-5, IPSL-CM6A-LR) and their ensemble. The model demonstrated high predictive accuracy (AUC = 0.67 training, 0.715 testing). Key factors included mean annual temperature, spring and autumn precipitation, slope, soil class and TRASP. Currently, 26.7% of the provinces are unsuitable, while 31.7% is highly suitable. Under future scenarios, unsuitable areas are projected to expand. The ensemble projects suitable area (Moderate, High, Very High) decreasing from 56.1% (baseline) to 50.7% under SSP1-2.6 and 52.0% under SSP5-8.5. However, substantial uncertainty exists across models under SSP1-2.6 (suitable area range: 44.5–52.9%; SD = ±3.1%), while model agreement is tighter under SSP5-8.5 (SD = ±1.0%). The greatest reduction is projected by MPI under SSP1-2.6 (−20.8%). These findings provide essential insights for adaptive strategies including crop redistribution, supplemental irrigation, and rainwater harvesting.

Key Words: CMIP6, MaxEnt, Rain-fed, Spatial Distribution.

1. Introduction

Rain-fed agriculture, which depends solely on natural precipitation, is highly vulnerable to climate change impacts such as rising temperatures and altered rainfall patterns (Rockström et al., 2010; Alegría et al., 2022; Manida, 2022). This vulnerability is particularly critical in semi-arid and dry sub-humid regions where irrigation options are limited (Wani et al., 2009; Rockström & Falkenmark, 2015). Assessing the spatial distribution of rain-fed agriculture and its climatic determinants is therefore essential for future land-use planning under global warming.

[1] Research Institute of Meteorology and Atmospheric Science, Climatological Research Institute (CRI), Mashhad, Islamic Republic of Iran.

At the global scale, several studies have mapped rain-fed cropland suitability using agro-ecological zoning or machine learning. For instance, Müller et al. (2021) modeled global rain-fed crop potential and found that 45% of current rain-fed areas face climate-induced suitability decline by 2050. Portmann et al. (2010) quantified rain-fed versus irrigated areas globally, highlighting that semi-arid regions have the highest interannual yield variability. Regionally, in East Asia, Liu et al. (2015) and He & Zhou (2016) projected northward shifts in rain-fed maize suitability under climate change. In Africa, Kogo et al. (2019) and Ali et al. (2023) identified growing season precipitation as the dominant predictor for rain-fed wheat. Synthesizing these studies, three consistent findings emerge: (1) precipitation during the growing season is the most critical driver, (2) semi-arid regions are hotspots of suitability loss, and (3) MaxEnt outperforms other SDMs for rain-fed applications due to its handling of presence-only data (Phillips et al., 2006).

Species Distribution Modelling (SDM) provides useful tools for this purpose by linking species occurrence data with climate and environmental predictors (Guisan & Thuiller, 2005; Elith et al., 2006; Sun & Liu, 2010). Among SDM approaches, the Maximum Entropy (MaxEnt) model has demonstrated high predictive accuracy and robustness, even with limited or biased datasets (Phillips et al., 2006; Fois et al., 2018; Rahimian Boogar et al., 2019). Its advantages, including flexibility with data types and production of response curves, have led to its wide application in assessing land suitability for major crops such as rice, maize, and wheat under both current and projected climate conditions (Ali et al., 2024; Feng et al., 2021; Yue et al., 2019).

Future projections of crop suitability often rely on General Circulation Models (GCMs), which simulate Earth's climate system with high precision (Kochkov et al., 2024; Moges & Moges, 2019). The Coupled Model Intercomparison Project Phase 6 (CMIP6) provides advanced climate projections under Shared Socioeconomic Pathways (SSPs), enabling the assessment of multiple development and climate scenarios (Eyring et al., 2016; O'Neill et al., 2016; Touzé-Peiffer et al., 2020; Tebaldi et al., 2021; Carvalho et al., 2022; Yang & Huang, 2023). Using GCM–MaxEnt integration, previous studies have projected shifts in crop suitability across regions such as East Asia and Africa, with findings highlighting significant risks to food security and the need for adaptive strategies (Liu et al., 2015; Ji et al., 2018; He & Zhou, 2016; Li et al., 2022; Kogo et al., 2019; Ali et al., 2023; Heng et al., 2024).

Although the MaxEnt model has been applied to ecological and agricultural research in Iran (Mahmoodi et al., 2022; Zarabian et al., 2023), no studies have yet evaluated rain-fed farming suitability in Qazvin Province.~~ Within Iran, MaxEnt has been used for rain-fed barley suitability in Fars province (Mahmoodi et al., 2022) and for almond wild relatives in Zagros forests (Zarabian et al., 2023). However, a systematic review of the literature reveals that no rain-fed cropland

suitability study exists for Qazvin Province or the broader Alborz southern foothills. This gap is surprising because: Despite covering only 1% of Iran's land area, this province contributes nearly 4% of national agricultural production, with the fertile Qazvin Plain playing a central role in wheat cultivation. Identifying present and future rain-fed cropland suitability under climate change scenarios in this region is thus of critical importance for sustainable agricultural planning.

Beyond just climate risks, Qazvin Province is also dealing with a range of human-driven pressures that are taking a toll on agricultural sustainability. Groundwater levels in the Qazvin aquifer have dropped nearly 20 meters over the past two decades, with the eastern and central plains hit hardest (Azadeh Ranjbar et al., 2025; Hashemi et al., 2023). Around 28% of the Qazvin Plain is now affected by high or very high levels of land degradation, and land use appears to be a major factor behind it (Contribution of predictive factors of land degradation, 2024). Rapid urbanization has also played a big role—built-up areas have increased by 67% since 1990, eating directly into agricultural land and green spaces. Meanwhile, traditional orchards, which help recharge the aquifer naturally, have shrunk by nearly 16% in recent years. All these pressures add up, making Qazvin Province not just an important agricultural region—it contributes 2.17% of the country's value-added from just 0.986% of its land—but also a critical place to study how rain-fed cropland might hold up under future climate change (Abolhasani et al., 2024; Sadeghi et al., 2025).

This study provides the first systematic assessment of rain-fed cropland suitability in Qazvin Province under current and projected climate conditions. While global studies (Zabel et al., 2014) have identified semi-arid Iran as potentially vulnerable, and national studies (Mahmoodi et al., 2022) have examined other provinces, no study has specifically addressed Qazvin—a region where high agricultural productivity collides with rapid groundwater depletion and land degradation. The novelty lies in: (1) identifying key climatic/environmental drivers specific to rain-fed agriculture in this understudied region, (2) quantifying current suitable land area at 1 km resolution, (3) mapping spatial changes under multiple climate scenarios (SSP2-4.5 and SSP5-8.5), and (4) discussing suitability shifts in the context of concurrent anthropogenic pressures. The specific objectives of this study are as follows:

- Identify the key climatic and environmental factors influencing rain-fed cropland distribution in Qazvin Province.
- Determine the proportion of land area suitable for rain-fed agriculture under current conditions.
- Evaluate spatial changes in suitable cultivation areas under SSP1-2.6 and SSP5-8.5 (2021–2040).

The results aim to offer practical insights for policymakers and agricultural planners to enhance resilience and ensure sustainable food production in Iran.

2. Material and methods

2.1. Study area

Qazvin Province (Figure 1), situated on the southern slopes of the Central Alborz Mountains in north-central Iran, encompasses diverse climatic zones shaped by topographic variation. Its climate ranges from cold and very cold conditions in the northern and southwestern highlands, to temperate zones in foothills, arid and semi-arid conditions across the central Qazvin Plain, and semi-humid to humid climates in the northeastern Alamut region. Annual precipitation varies from approximately 210 mm in the east to over 700 mm in the northeastern highlands, with maximum values recorded in Alamut and Avaj. Mean annual temperatures range between 12–14 °C, with the lowest values in highland areas and the highest in the central plain and around Manjil Dam Lake. The land use distribution across Qazvin Province, encompassing rangelands, rain-fed croplands, irrigated agriculture, highly saline lands with no vegetation cover, and orchards. Wheat is cultivated both as rain-fed and irrigated crops; approximately 70% of the total wheat cultivation area is allocated to rain-fed wheat, covering about 90,000 hectares in 2024. Among the counties, Avaj and Takestan possess the largest areas under rain-fed agriculture.

Qazvin Province covers only 0.986% of Iran's total land area. However, it generates 2.17% of the country's agricultural value-added and contains 2.99% of its total cropland (including both irrigated and rain-fed systems). This disproportionate agricultural productivity, particularly in rain-fed wheat cultivation, makes the province a critical yet understudied region for climate-adaptive land-use planning.

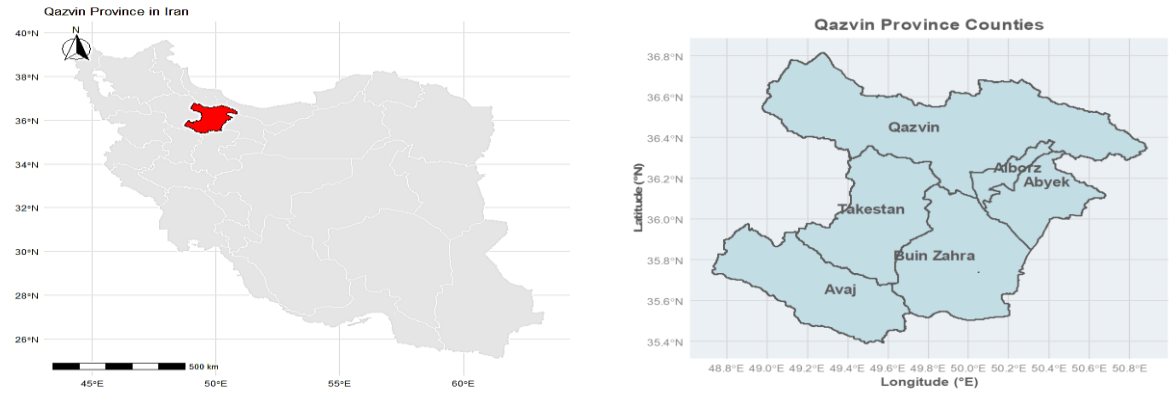

Figure 1. location of Qazvin Province in Iran (highlighted in red) within Iran (left), Location map of Qazvin Province showing its six counties (right).

2-2. Environmental modeling data

Two primary datasets are required for constructing the model. The first dataset includes the spatial distribution data of the target species—in this case, a shapefile of rain-fed cropland—obtained from the Planning and Management Organization of Qazvin Province. The second dataset consists of nine selected climatic and topographic variables that are considered to significantly influence the distribution of rain-fed cropland. We selected these because they directly or indirectly affect soil moisture, crop growth, and overall agricultural suitability in rain-fed environments (IPCC, 2014; Hatfield & Prueger, 2015; Rockström et al., 2010; FAO, 2018). Topographic variables strongly shape the spatial distribution of rain-fed cropland in Qazvin through their influence on microclimatic and hydrological conditions. Elevation determines temperature, frost, and precipitation gradients, thereby defining agro-ecological zones (Dobrowski et al., 2013). Slope steepness regulates surface runoff, with steeper slopes (>5%) intensifying soil moisture loss and constraining crop growth (Tesfay, 2020). Studies indicated that slope is essential for soil stability and water retention; mild to moderate slopes (0–15%) are ideal because they minimize runoff and erosion risks while balancing drainage and infiltration (Mu et al., 2015). Since the growing season peaks in the spring, precipitation is especially crucial for rain-fed crops like wheat and barley. The finding that parameters linked to precipitation are crucial for rain-fed cropland suitability is consistent with earlier studies that found precipitation to be a crucial determinant in marginal production systems (Nogueira et al., 2024; Gao et al., 2020). Aspect further modifies solar insolation and wind exposure, where north-facing slopes retain more moisture, enhancing suitability for rain-fed systems (Bennie et al., 2008). While solar radiation is critical for photosynthesis, its variability is adequately represented by elevation and aspect, and water availability remains the primary limiting factor in rain-fed agriculture (Elith et al., 2011).

We pulled climate data from WorldClim version 2.1, which offers 2.5 arc-minute resolution (about 4.4 km) for the historical period of 1985 to 2014. WorldClim is a well-known, freely available source of high-resolution climate data that's widely used in agricultural and ecological modeling, as well as species distribution studies (He et al., 2012; Ali et al., 2023). The climate variables we chose (listed in Table 1) include mean annual temperature (°C), along with mean annual precipitation and seasonal precipitation for autumn, winter, and spring (mm).

We also brought in soil characteristics—especially texture and depth—using the SoilGrids database (ISRIC, www.isric.org), which provides globally consistent estimates of soil properties across six depth layers down to 200 cm. For topographic variables like elevation, slope, and aspect, we used the SRTM DEM at 30-meter resolution and then averaged them up to match the climate data resolution using the mean function in R's terra package. Instead of using raw aspect, we went with

the Topographic Radiation Aspect Index (TRASP), which was proposed by Roberts and Cooper (1989). TRASP is a straightforward linear transformation of aspect, calculated as:

$$\text{TRASP} = \frac{1-\cos\left(\frac{\pi}{180}(\text{Aspect}-30)\right)}{2} \quad (1)$$

This index maps aspect to a continuous scale from 0 to 1, where 0 represents the coolest, wettest orientations (north-northeast) and 1 represents the hottest, driest orientations (south-southwest). This transformation is more physically meaningful for our rain-fed cropland suitability assessment because it directly correlates with solar radiation and soil moisture gradients. By using TRASP instead of aspect, the MaxEnt model can more accurately capture the ecological reality that south-facing slopes in the northern hemisphere are less suitable for rain-fed agriculture due to higher evapotranspiration. All layers were harmonized to identical extent, resolution (4.4 km), and coordinate system (WGS84).

Table 1. Independent climatic and environmental variables with their references.

Variable name	Source	Unit	Type	Traceable Reference (with DOI/access date)
Aspect	http://www.earthenv.org/topography	%	Environmental	Amatulli, G., et al. (2018). EarthEnv-D90: A global elevation gradient dataset. Scientific Data. DOI: 10.1038/sdata.2018.102 (Access: earthenv.org/topography, downloaded [date])
Slope	http://www.earthenv.org/topography	Degree	Environmental	Amatulli, G., et al. (2018). EarthEnv-D90: A global elevation gradient dataset. Scientific Data. DOI: 10.1038/sdata.2018.102 (Access: earthenv.org/topography, downloaded [date])
Elevation	http://www.earthenv.org/topography	m	Environmental	Amatulli, G., et al. (2018). EarthEnv-D90: A global elevation gradient dataset. Scientific Data. DOI: 10.1038/sdata.2018.102 (Access: earthenv.org/topography, downloaded [date])
Mean annual temperature , Mean annual precipitation, Mean seasonal precipitation (winter, autumn and spring)	www.worldclim2.org (Fick & Hijmans, 2017)	mm	Climatic	Fick, S.E., & Hijmans, R.J. (2017). WorldClim 2: New 1-km spatial resolution climate surfaces for global land areas. *International Journal of Climatology*, 37(12), 4302-4315. DOI: 10.1002/joc.5086 (Variable: bio1). December-January-February (prec_12, prec_01, prec_02)
Soil	https://soilgrids.org/	class	Soil type	Poggio, L., et al. (2021). SoilGrids 2.0: producing soil information for the globe with quantified spatial uncertainty. *SOIL*, 7(1), 217-240. DOI: 10.5194/soil-7-217-2021

This study used downscaled output from the three GCMs (Table 2) of CMIP6 for the years 2021–2040, which are available at http://worldclim.org/cmip6, to project the future area suitability for rain-fed agriculture. Hereafter, these models are referred to as MPI, ACCESS, and IPSL.

Table 2. Three GCM from CMIP6 models used in this study.

Research Centre	Country	Global Climate Model	Grid resolution (lat, lon)
Max Planck Institute for Meteorology (MPI-M)	Germany	MPI-ESM1-2-LR	1.39° x 1.41°
Commonwealth Scientific and Industrial Research Organisation (CSIRO)	Australia	ACCESS-ESM1-5	1.25° x 1.875°
The Institute Pierre-Simon Laplace Climate Modeling Center	France	IPSL-CM6A-LR	2.5° x 1.25°

2-3. MaxEnt modeling approach

The MaxEnt model estimates the conditional probability distribution P(y|x), where x denotes the set of environmental predictor variables and y corresponds to the occurrence (presence) of a species. The objective of this model is to find a probability distribution P(y|x) that maximizes entropy while remaining consistent with the empirical expectations derived from the environmental characteristics of the observed presence records (Eq. 1)

$$P(y|x) = \frac{1}{Z(x)} \exp\left(\sum_i \lambda_i f_i(x|y)\right) \quad (2)$$

In this context, $f_i(x|y)$ represents the feature functions that describe the relationships between variables x and y. The coefficients λ_i are the feature weights estimated during the training process. Additionally, $Z(x)$ denotes the normalization constant defined by Equation (2):

$$Z(x) = \sum_y exp\left(\sum_i \lambda_i f_i(x|y)\right) \quad (3)$$

This model works entirely with presence data—essentially, where something has been observed—and uses a set of environmental factors to tell the difference between those occurrence records and the broader landscape (Akpoti et al., 2020). By relying on presence-only data alongside background environmental information, MaxEnt helps reduce the problems that come with incomplete datasets and avoids overfitting by using regularization techniques. The end result is a continuous probability map that shows suitability. From there, you can apply thresholds to turn that map into simple presence-absence predictions or different suitability classes. The model also comes with some handy tools, like jackknife tests, species response curves, and evaluation metrics such as the Area Under the ROC Curve (AUC) and the ROC curve itself. It can be run either through an easy-to-use graphical interface or via command-line tools (Merow et al., 2013). For this study, the MaxEnt model was built using the "raster" and "dismo" packages in R.

Distribution modeling using highly correlated bioclimatic data can affect the predicting process and overestimate distributions (Hijmans et al., 2005, Ali et al., 2023; Braunisch et al., 2013). In this

study, to ensure the reliability and interpretability of the MaxEnt model, the multicollinearity among predictor variables was assessed using the Variance Inflation Factor (VIF). VIF quantifies how much the variance of a regression coefficient is inflated due to multicollinearity with other predictors. A VIF value of 1 indicates no correlation between a given predictor and any others. As VIF increases, it suggests a higher level of collinearity. Common interpretive thresholds are VIF > 5 for moderate and VIF > 10 for severe multicollinearity (Guisan & Zimmermann, 2000, Akinwande et al., 2015) (Figure 2).

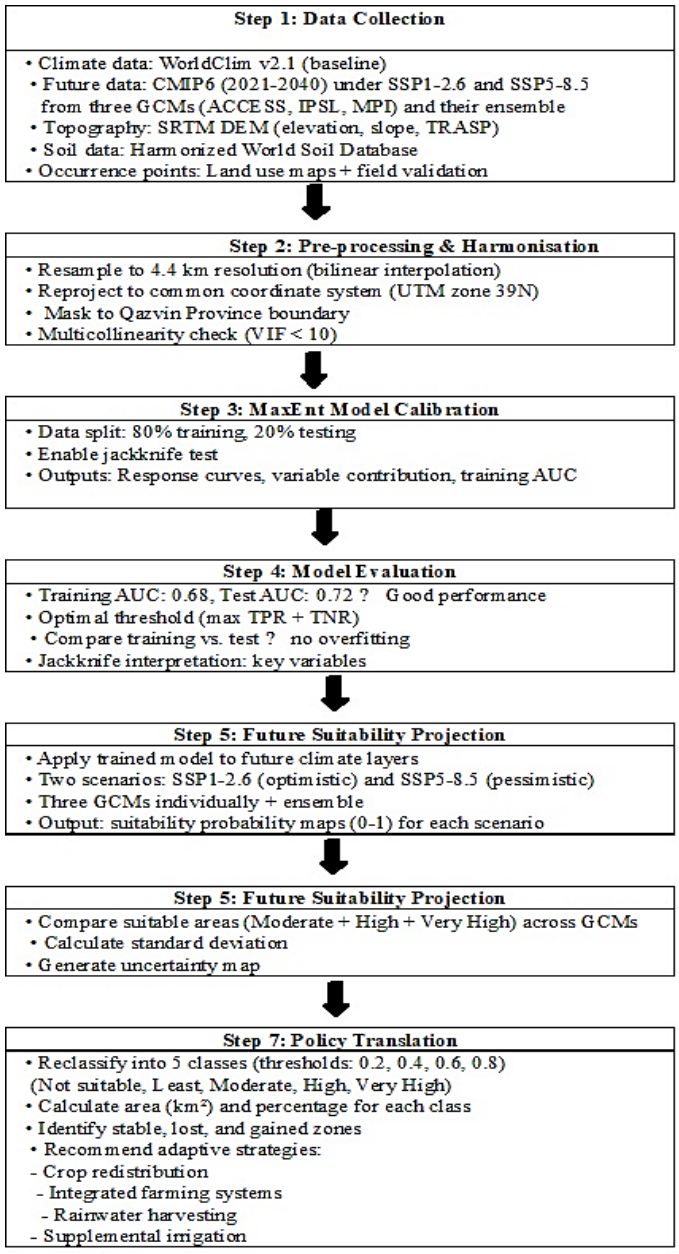

Figure 2. Methodological flowchart for assessing rain-fed cropland suitability in Qazvin Province under current and future climate scenarios (SSP1-2.6 and SSP5-8.5).

3. Results

3.1. Predictor variable selection and multicollinearity assessment

The performance and transferability of species distribution models (SDMs) depend on several ecological, biological, and methodological factors (van Steenderen & Sutton, 2024). However, these variables often exhibit high collinearity, and most statistical approaches require selecting one variable from among those that are strongly correlated. In this study, the strength of correlation between independent variables was assessed using the Pearson correlation coefficient. The results indicated that mean annual precipitation (Annual_Prec) was highly correlated with mean autumn (Autumn_Prec) and winter (Winter_Prec) precipitation (r = 0.98 and r = 0.89, respectively). Mean annual temperature (Annual_Tem) showed a correlation of -0.94 with elevation, and mean autumn precipitation had a correlation of approximately 0.93 with mean winter precipitation (the results are not shown).

The collinearity test, VIF results revealed that among the nine variables, mean annual precipitation, mean winter precipitation and elevation exhibited high correlation and VIF values greater than 10, making them suitable for removal. After removing the collinear variables, The absolute magnitudes of the linear correlation coefficients fell within a range of 0.02 (TRASP ~ mean spring precipitaion) to a maximum of 0.56 (mean annual temperature ~ mean autumn precipitation). Consequently, the model was run using six raster layers: slope, soil class, mean annual temperature, TRASP, soil, mean spring and autumn precipitation (Figure 3).

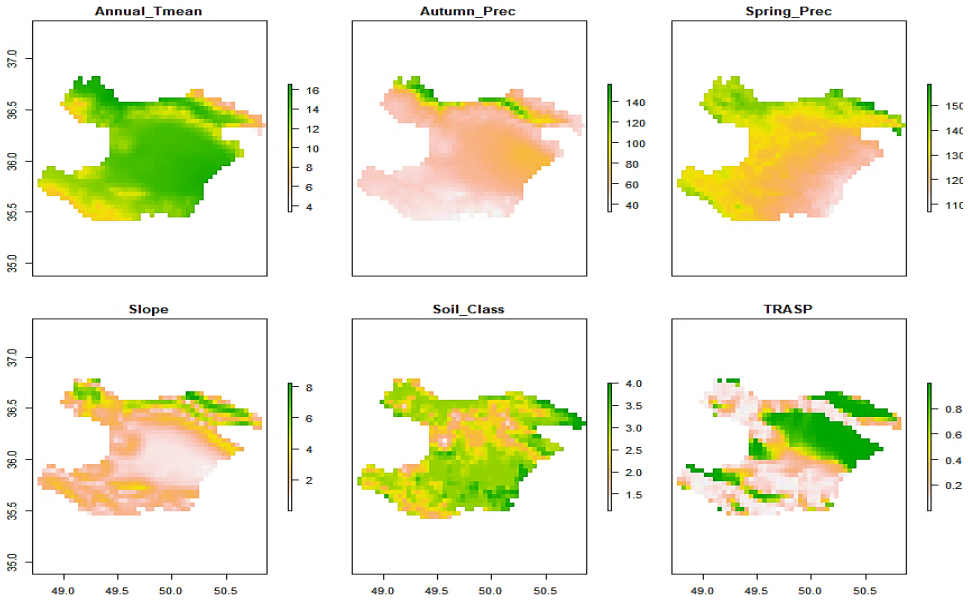

Figure 3. Raster layers of the selected climatic and topographical predictors used in the MaxEnt model for rain-fed cropland suitability assessment in Qazvin Province: mean annual temperature (°C), autumn precipitation (mm), spring precipitation (mm), slope (%), soil class, and (f) TRASP index (0 = cool/wet, 1 = hot/dry). All layers were resampled to 4.4 km resolution and share the same spatial extent.

3.2. Model Performance and Validation

To implement the MaxEnt model, 80% of the dataset was utilized as training data to construct the model and estimate its parameters, while the remaining 20% was reserved for evaluating the model's performance.

The ROC curves for our training and test data gave us AUC values of 0.68 and 0.72, respectively (Hanley, 1989). Now, these numbers fall somewhere between the "poor" (0.6–0.7) and "good" (0.7–0.8) ranges, but they're actually pretty comparable to—or even better than—many published crop suitability models that only rely on climate and topography. What's interesting is that the test AUC was slightly higher than the training AUC (0.68 to 0.72). That's a good sign—it means the model isn't overfitted, and it might actually do a slightly better job predicting on new data than it did on the data it was trained on.

We see these scores as evidence of moderate but practically useful predictive power. In the real world, human factors like land tenure, input availability, and market access play a huge role in where crops are actually grown. So hitting an AUC above 0.7 is pretty reasonable and acceptable for our purposes. The model captures the main biophysical patterns well enough to help guide regional planning, even if it can't predict every single field with high precision.

For evaluation, we tested the MaxEnt model on an independent dataset of 1,391 presence points and 892 random background points. It achieved a test AUC of 0.731 (Figure 4), which tells us the model does a good job distinguishing suitable from unsuitable rain-fed cropland areas. The correlation between predicted and observed values came out to 0.443 a moderate positive relationship. We found the optimal probability threshold to be 0.563, balancing sensitivity and specificity as best as possible. At that threshold, the model correctly identified about 40.1% of suitable locations (that's the sensitivity). The full range of predicted suitability probabilities went from 0.17 to 0.93, so the model is picking up both low and high suitability areas across the province.

All in all, while the model shows solid discrimination ability (AUC over 0.73), the fairly low sensitivity at the optimal threshold does mean that some suitable areas aren't captured with high confidence. But that's a common challenge in agricultural suitability modeling—human decisions like land tenure and market access often get tangled up with biophysical conditions, making perfect prediction tough (Tapas et al., 2025).

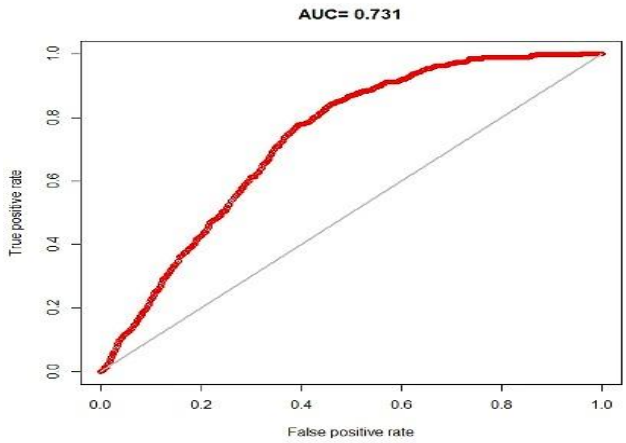

Figure 4. Receiver Operating Characteristic (ROC) curve for the MaxEnt model evaluated on the independent test dataset.

3.3. Variable Contributions and Response Curves

The contributions and importance of each of the six predictors were analyzed using the jackknife test (Phillips et al., 2006). The results showed that slope, mean annual temperature, and mean spring precipitation consistently stood out as the top three variables, with similar influence patterns in both training and test datasets (Figure 5).

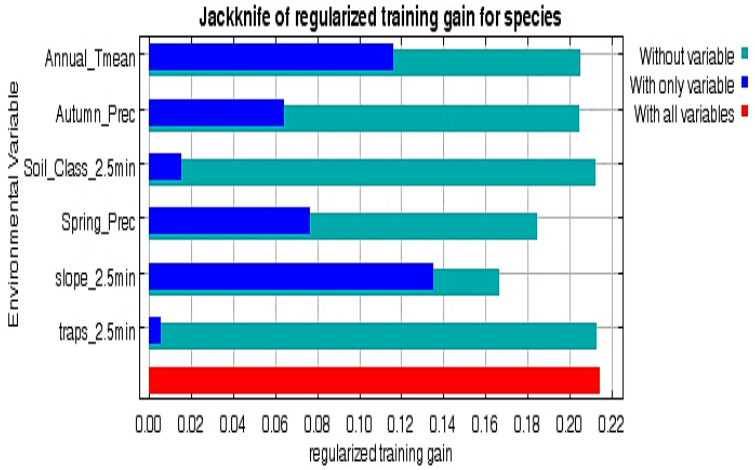

Figure 5. Jackknife test results for the six environmental variables. Blue bars show model gain using only the specified variable. Green bars show model gain when that variable is excluded from the full model.

In figure 5, the blue bars show how much predictive power the model gains when each variable is used by itself, while the green bars show what happens when that variable is taken out of the full model. The red line marks the full model's overall gain, which sits at 0.21. Slope really stands out. When used alone, it achieved the highest gain at 0.13—actually edging past the full model's performance. Mean annual temperature came next with a gain of 0.11, followed by spring

precipitation at 0.07 and autumn precipitation at 0.06. Soil class and TRASP didn't do much on their own, with gains of just 0.04 and 0.02 respectively. When each variable was removed from the full model (green bars), the gain increased for all variables — indicating that the full model may be slightly overfitted. The smallest increase happened when we removed slope (from 0.13 to 0.17), which tells us slope contributes the most unique information that the other variables just don't capture. On the flip side, removing soil class or TRASP caused the biggest jump (up to 0.20), meaning those variables aren't adding much unique value. Honestly, we could probably drop them from a simpler version of the model.

The jackknife test confirms that slope, mean annual temperature, and spring precipitation are the three most important predictors for rain-fed cropland suitability in Qazvin Province. Slope is both the strongest individual predictor and carries the most unique information. And that makes practical sense—gentle slopes hold onto water, while steep slopes lose it fast. That's a real, on-the-ground constraint for farmers trying to grow rain-fed crops. Mean annual temperature being important isn't surprising either, given this is a mountainous, semi-arid region. But spring precipitation really stood out for its critical role during grain filling—a dry spring can literally wipe out an entire harvest. Autumn precipitation plays more of a threshold role: even if the rest of the year looks wet, too little rain in autumn means seeds just won't germinate. Soil class and TRASP? They barely contribute, so we might consider dropping them in future model updates. This pattern lines up nicely with earlier studies that highlighted precipitation as a key factor (He et al., 2012; Ali et al., 2023). TRASP and soil class just didn't add much to the provincial scale. That doesn't mean they're irrelevant everywhere—locally, they might matter—but across Qazvin as a whole, slope and temperature are clearly driving where rain-fed farming is feasible. For four out of the six variables, the difference between training and test contributions was less than 8%. That's a good sign that the model isn't overfitted and that these key drivers should hold up outside our study area (we didn't show those results here).

3.4. Current Rain-Fed Cropland Suitability

The MaxEnt model output for rain-fed cropland in Qazvin Province was classified into suitability classes based on the presence probability (p). Many SDM studies have employed a prediction probability threshold of 0–0.2 to identify areas unsuitable for rain-fed cropland. This classification aids in extracting finer details regarding rain-fed cropland predictions within a geographical context (Li et al., 2023). Consequently, this study utilizes five equal-sized probability classes, each with a threshold of 0.2. These classes are defined as follows: 5 = very high land suitability ($p > 0.8$); 4 =

high suitability ($0.6 > p \leq 0.8$); 3 = moderate suitability ($0.4 > p \leq 0.6$); 2 = low suitability ($0.2 > p \leq 0.4$); and 1 = no suitability ($p < 0.2$).

Figure 6 presents the spatial distribution of five rain-fed cropland suitability classes across Qazvin Province, revealing a clear north–south gradient with distinct geographical patterns and policy implications. Very high suitability areas (dark green), covering 11.1% of the province (1,853.8 km²), are predominantly located in the central and western portions, extending across gentle slopes characterized by favorable temperature regimes and adequate spring precipitation. Specifically, these areas include parts of Tarom-e Sofla, Ziaabad, and Alamut-e Gharbi districts, where low to moderate slopes and well-timed seasonal precipitation together support viable rain-fed cropping. High suitability areas (green) account for 31.7% of the total area and extend into parts of central Qazvin Province around Qazvin city and southern Alborz County. Although still favorable, these zones experience slightly lower precipitation and higher temperatures compared to the very high suitability zone, with a moderate risk of moisture stress in some years. Rain-fed farming remains feasible here under good management practices, including drought-tolerant varieties, early-maturing cultivars, and soil conservation measures such as no-till farming. Moderate suitability areas (light green) form a transitional belt between the suitable and unsuitable zones, covering much of the central Qazvin Plain. Rain-fed farming is possible in these areas but carries significant drought risk during low-rainfall years. Farmers may achieve good yields in wet years but face complete crop failure in dry years. Policy interventions in these zones should therefore prioritize risk management strategies, including crop insurance, fodder reserves, and livelihood diversification. Integrated farming systems—combining rain-fed crops with small livestock—offer improved resilience in this context. Taken together, the moderate, high, and very high suitability classes represent just over half of the province (56.1%), indicating that a substantial portion of Qazvin Province is potentially suitable for rain-fed farming under current climatic conditions. Least suitable areas (cream) are concentrated in the southern and southeastern parts of the province, particularly in Buin Zahra, Abyek, and eastern Takestan. Low rainfall combined with higher temperatures—leading to increased evapotranspiration—makes rain-fed wheat farming very risky, with yields approaching zero in below-average rainfall years. In these marginal areas, policymakers should seek livelihood alternatives such as a transition to irrigated agriculture, greenhouse production, or sustainable livestock farming. Continued rain-fed farming without systemic changes (e.g., rainwater harvesting) is not economically viable. Finally, not suitable areas, covering 26.7% of the study area (4,435.2 km²), appear as scattered patches in the southern lowlands (especially southern Buin Zahra and Abyek) as well as in some western and eastern areas. Climatic and topographic conditions—very low rainfall, high seasonal temperatures, and occasionally steep

slopes—make any successful rain-fed farming impossible here. Wheat cultivation is only feasible under full irrigation. Rain-fed farming has no justification in these areas, and policy should focus exclusively on irrigated agriculture or non-agricultural land uses, such as sustainable rangeland management or solar energy development.

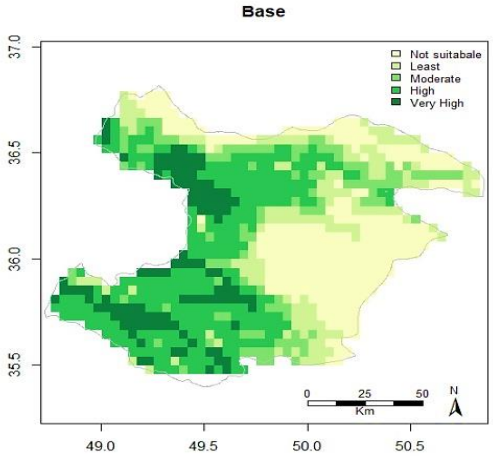

Figure 6. The spatial distribution of five classes of land suitability for rain-fed cropland in Qazvin Province during base period.

3.5. Projecting of the climatic predictors under SSP scenarios

Table 3 presents a comparative overview of historical climate conditions in Qazvin Province (1984–2014) alongside projected near-future conditions (2021–2040) under two contrasting pathways: a low-emission scenario (SSP1-2.6) and a high-emission scenario (SSP5-8.5).

Spring precipitation represents a critical period for rain-fed wheat, coinciding with the grain-filling stage. Historically, spring rainfall across the province ranged from 106 to 158 mm. Model ensembles project a modest increase, with values reaching 107–160 mm under SSP1-2.6 and 109–162 mm under SSP5-8.5. While not dramatic, this slight improvement could offer meaningful benefits during a key phenological stage.

Autumn precipitation tells a somewhat different story. Historically, autumn rainfall has been highly variable, ranging from as low as 32 mm to as high as 156 mm. This wide interannual variability implies that some autumns are severely dry, while others are relatively generous. What stands out in the future projections is not the upper bound but the lower bound. Under both scenarios, the driest autumns are expected to become less dry, with the minimum increasing from 32 mm historically to approximately 40–42 mm. Although this increase may appear modest, for farmers relying on autumn rains to germinate their crops, such a shift could meaningfully reduce the risk of planting failure.

Temperature exhibits a clear and consistent warming signal across all models. Historically, mean annual temperatures in Qazvin Province ranged from approximately 3.3°C in the cooler highlands to 16.6°C in the warmer lowlands. By the 2021–2040 period, under SSP1-2.6, this range is projected to shift to 4.4–17.6°C, corresponding to a warming of roughly 1.1°C. Under the high-emission SSP5-8.5, temperatures are expected to reach 4.6–17.8°C, representing an increase of about 1.3°C. Notably, individual models diverge in their projections. The ACCESS model consistently projects the strongest warming, with upper temperatures reaching 18.3°C under SSP5-8.5. The same model also stands out for its projections of the largest increases in spring precipitation, up to 171 mm under the high-emission scenario. These inter-model differences underscore an important point: the future is not deterministic. What we work with are ranges and probabilities, not precise predictions. Substantial uncertainty remains inherent in the projections, arising primarily from differences in the physical parameterizations, boundary conditions, and climate sensitivities of the individual GCMs employed.

Table 3. Uncertainty in projected climatic predictors over Qazvin Province based on outputs of GCMs under two SSP scenarios during the baseline and near-future periods

Predictor	Base	MPI		ACCESS		IPSL		Ensemble	
		SSP1-2.6	SSP5-8.5	SSP1-2.6	SSP5-8.5	SSP1-2.6	SSP5-8.5	SSP1-2.6	SSP5-8.5
Mean spring precipitation (mm)	106-158	101-156	107-162	110 - 162	115 - 171	110 - 162	107-154	107 - 160	109- 162
Mean autumn precipitation (mm)	32 – 156	41 - 150	41-146	40 - 144	42 - 142	42 - 145	41- 142	41 - 146	41 - 143
Mean annual temperature (°C)	3.3 – 16.6	3.9-17.1	4-17.2	4.9 - 18.1	5 – 18.3	4.6 – 17.8	4.8 – 18	4.4 – 17.6	4.6 – 17.8

3.6. Future Suitability under SSP Scenarios

Due to space constraints in the main manuscript, the individual suitability maps for the three GCMs (ACCESS, IPSL, and MPI) are not presented here. However, the uncertainty across these models is quantified in Table 4, which reports the projected suitable area (combining the Moderate, High, and Very High suitability classes), the corresponding percentage of the provincial area, the percentage change relative to the baseline period, and the standard deviation for each GCM and their ensemble under both SSP scenarios. Under the low-emission scenario (SSP1-2.6), the ensemble projects a suitable area of 8,420 km², equivalent to 50.7% of the province, representing a −9.8% change relative to the baseline period. However, model disagreement is considerable, with a standard deviation of ±522.8 km². Notably, the MPI model projects a steep decline of −20.8%, whereas IPSL projects a more modest reduction of −5.8%. Under the high-emission scenario (SSP5-8.5), the ensemble projects a suitable area of 8,645 km² (52.0% of the province, −7.4% change from baseline). In contrast to the low-emission scenario, inter-model agreement is

substantially higher here, with a standard deviation of only ±173 km². This somewhat counterintuitive finding suggests that under a high-emission pathway, the strong and consistent warming signal may overwhelm model-specific disagreements regarding precipitation changes, leading to more certain projections of suitable area loss.

Tabel 4. Uncertainty in projected suitable area across three GCMs (ACCESS, IPSL and MPI) along with an ensembel of these models under SSP5-8.5 and SSP1-2.6.

	SSP126			SSP858		
GCM	Suitable area (km^2)	% of Province	% Change	Suitable area (km^2)	% of Province	% Change
ACCESS-ESM1-5	8437.275	50.8	-9.6	9078.3	54.6	-2.8
IPSL-CM6A-LR	8801.1	52.9	-5.8	8801.1	52.9	-5.8
MPI-ESM1-2-LR	7397.775	44.5	-20.8	8662.5	52.1	-7.2
Ensembel	8419.95	50.7	-9.8	8645.175	52	-7.4
Standard deviation	±522.81	±3.1	±5.6	±173.4	±1.04	±1.9

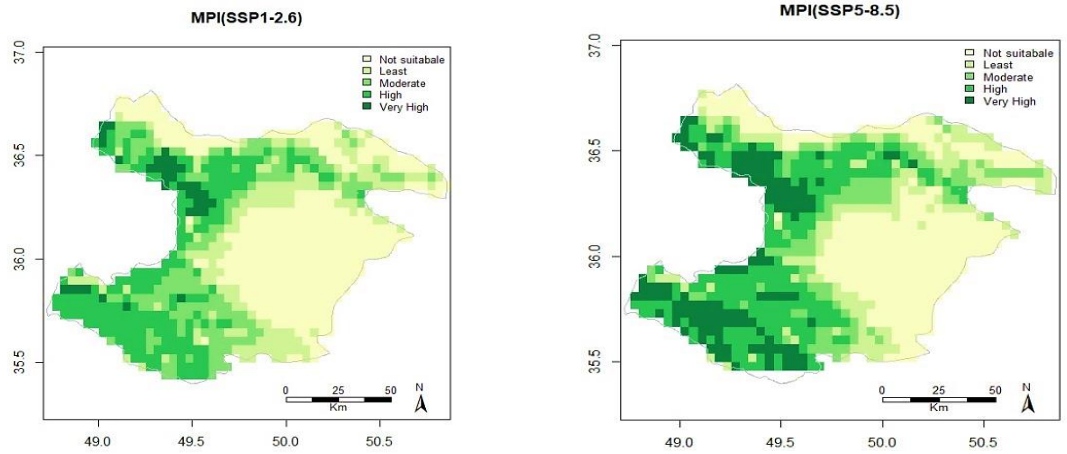

Figure 7. Spatial distribution of rain-fed cropland suitability in Qazvin Province under (a) baseline conditions, (b) SSP1-2.6 (MPI), and (c) SSP5-8.5 (MPI).

Given the steep decline simulated by the MPI model under future scenarios, Figure 7 presents the spatial distribution of rain-fed cropland suitability classes in Qazvin Province under two specific combinations: SSP1-2.6 (low emissions) and the MPI model under SSP5-8.5 (high emissions). This comparison is designed to identify locations most vulnerable to the projected reduction. Contrary to what might be expected, the MPI model projects a larger suitable area under the high-emission scenario (52.1% of the province) than under the low-emission scenario (44.5%). Under SSP1-2.6, the suitable area contracts to just 44.5% of the province, a decline of 20.8% relative to the baseline period. Under this scenario, the Moderate, High, and Very High suitability zones are likely restricted to a narrow belt along the northern Alborz foothills, while the central and southern plains become predominantly unsuitable. This pattern reflects MPI's projection of relatively dry conditions

under low emissions. Under SSP5-8.5, however, the suitable area remains at 52.1% of the province, a decline of only 7.2% from baseline. Notably, the suitable zone expands further south compared to SSP1-2.6, suggesting that the MPI model simulates sufficient increases in spring and/or autumn precipitation under high emissions to partially offset the warming-driven rise in evapotranspiration. This counterintuitive result highlights a critical source of uncertainty in climate impact assessments: different GCMs simulate different relationships between warming and precipitation. In the case of MPI, higher emissions bring more rain, which in turn benefits rain-fed agriculture. However, as shown in Table 4, this pattern is not consistent across all models—IPSL, for example, exhibits markedly different behavior.

4. Discussion

This study examined the potential geographic distribution of rain-fed cropland of Qazvin province using MaxEnt model under the SSP1-2.6 and SSP5-8.5 scenarios, utilizing climatic variables from three CMIP6 models (MPI, ACCESS, and IPSL) and along with an ensembel of these models. The performance of the MaxEnt model confirmed its appropriateness for predicting climate and environmental suitability for rain-fed cropland. This is in agreement with the findings of related studies that found the model is applicable in assessing crop suitability (Duan and Zhou (2012); Machovina and Feeley (2013); Liu et al. (2015); Ji et al. (2018); Ali et al., (2023), and He and Zhou (2016).

The geographic suitability for rain-fed cropland in Qazvin Province is divided into five classes—Very High, High, Moderate, Least, and Not suitable, which, under current climate conditions, closely align with the actual distribution of rain-fed cropland across the province.

The spatial distribution map (Figure 5) reveals that the Very High and High suitability zones are concentrated in a northwest-to-southeast belt along the Alborz mountain foothills, together covering approximately 43% of the province. These areas represent the core of Qazvin's rain-fed wheat production system. In contrast, the southern and southeastern parts of the province, particularly Buin Zahra and Abyek counties, are predominantly classified as Least suitable or Not suitable, accounting for roughly 44% of the provincial area. Rain-fed wheat farming in these regions is highly risky even under current climate conditions, with frequent crop failure occurring during dry years. Agricultural policymakers should therefore consider the gradual relocation of rain-fed farming away from these southern areas toward the more favorable northern belt. The central belt, which includes portions of the Qazvin Plain, falls into the Moderate suitability class. Rain-fed farming is possible here but requires robust risk management, the use of drought-resistant varieties,

and optimal moisture conservation practices. These areas function as transition zones and are likely to be the first to drop out of rain-fed production under future climate change.

Among the GCMs evaluated, the MPI model presents an unusual but instructive case. It projects greater rain-fed cropland suitability under the high-emission SSP5-8.5 scenario than under the low-emission SSP1-2.6 scenario. This is not an error; rather, it reflects the precipitation changes simulated by MPI (Table 3). Under SSP5-8.5, MPI projects increases in spring and autumn precipitation large enough to offset the negative effects of warming on soil moisture. Under SSP1-2.6, by contrast, MPI projects drier conditions, leading to a sharper decline in suitability. This finding underscores a key message of our study: for rain-fed agriculture, the direction and magnitude of precipitation change is often more important than the direction of temperature change. Unfortunately, precipitation is also the variable over which GCMs disagree most strongly. Similar results have been reported in other MaxEnt-based studies. For example, Yue et al. (2019) found that climate change will benefit wheat cultivation in middle and high latitudes while threatening it in low latitudes.

4.1. Limitations and future research directions

Despite the novel contributions of this study, the first systematic assessment of rain-fed cropland suitability in Qazvin Province under SSP scenarios, several limitations must be acknowledged.

4.1.1 Uncertainties associated with climate data sources and downscaling

Several uncertainties arise from our use of WorldClim v2.1 (Fick & Hijmans, 2017). First, sparse weather station coverage in semi-arid regions of Iran increases interpolation uncertainty, particularly for precipitation. Second, aggregating the digital elevation model (DEM) to a coarser resolution result in the loss of fine-scale topographic information. This may lead to overestimation of suitable areas in heterogeneous terrain and reduce model sensitivity to important microtopographic features. Second, the delta downscaling method assumes that the statistical relationships between coarse- and fine-scale climate anomalies remain stationary over time, an assumption that may not hold in complex mountainous terrain. Fourth, the use of long-term means (1985–2014) masks inter-annual variability, including drought years that are critically important for rain-fed agriculture. Fifth, future projections inevitably inherit uncertainties from the underlying GCMs and the downscaling algorithms employed. We recommend that future studies address these limitations by incorporating local station data, utilizing regional climate models such as CORDEX-ME, and including inter-annual variability metrics.

4.1.2. Representativeness and generalizability

This study focuses solely on Qazvin Province, which accounts for only 0.986% of Iran's land area but contributes 2.17% of the country's agricultural value-added. The bioclimatic thresholds we derived, for example, an optimal precipitation range of 280–350 mm, are context-dependent and not directly transferable to larger or more heterogeneous regions, such as all of Iran. However, our methodological framework itself is transferable. Future studies should apply the same MaxEnt–CMIP6 workflow to adjacent provinces (e.g., Zanjan and Hamedan) or to the entire Alborz foothills belt to test the spatial robustness of our findings.

4.1.3. Anthropogenic pressures not included in the model

Our model identifies climatically suitable areas but does not account for ongoing anthropogenic pressures that significantly influence agricultural viability. Urban expansion is projected to convert 983 hectares to built-up land by 2025, primarily in the northern and eastern parts of the province (Sadeghi et al., 2025). Land degradation affects 27.7% of the Qazvin Plain, classified as high or very high severity (Abolhasani et al., 2024). Furthermore, groundwater levels have dropped by 20 meters between 2002 and 2022, with 15 meters of that decline occurring in the last three years alone (Azadeh Ranjbar et al., 2025), thereby reducing the capacity for supplemental irrigation during drought periods. Future research should integrate these pressure layers with climate suitability assessments to provide a more holistic picture.

4.1.4. Reliance on long-term mean climate variables

We used 30-year mean climate data from WorldClim v2.1, which does not capture inter-annual variability, including dry and wet extremes. In a semi-arid region like Qazvin, a "suitable" mean precipitation value, say, 300 mm per year, may in reality mask alternating sequences of very dry and very wet years, neither of which reliably supports rain-fed production. Future work should therefore incorporate drought frequency indices such as the Standardized Precipitation Index (SPI) or the Palmer Drought Severity Index (PDSI), use annual time-series data, and employ process-based crop models such as DSSAT or APSIM.

4.1.5. Nonstationarity of hydroclimatic variables

Climate nonstationarity, increasingly documented in Iran (Kousali et al., 2022), can lead to underestimation of drought risk (Zhang et al., 2022) and nonstationary crop yield responses (Wang et al., 2021). Future studies should therefore move beyond mean-based predictions and incorporate time-varying covariates along with inter-annual variability metrics.

5. Conclusions

Increasing temperatures and shifting precipitation patterns pose a serious threat to rain-fed cropland productivity. In Iran, Javadi et al. (2024) estimated that rain-fed wheat yields could decrease by 21% under an average emissions scenario. The suitability maps generated in this study provide a spatial decision-support tool for agricultural planning in Qazvin Province. However, translating suitability into actionable policy requires concrete intervention pathways, and international case studies offer tested models to guide this process.

First, strategic crop redistribution has proven effective elsewhere. Shi et al. (2024) demonstrated that optimizing wheat distribution at 1 km resolution reduced blue water consumption by 16%, the grey water footprint by 21%, and greenhouse gas emissions by 18%, while simultaneously improving irrigation water productivity by 21% and nitrogen use efficiency by 11%. For Qazvin, this finding implies that policymakers should consider gradually shifting rain-fed wheat cultivation away from areas projected to become unsuitable under the SSP5-8.5 scenario, particularly the southern low-elevation zones, toward areas with stable or improving suitability, such as the northern foothills. Such a transition could be facilitated through land-use incentives or strategic crop zoning.

Second, where rain-fed suitability declines substantially, modifying the cropping system offers a viable alternative to outright abandonment. In the Huang-Huai-Hai region of China, Wang et al. (2024) found that replacing the traditional winter wheat–maize rotation with a winter wheat–soybean rotation reduced water consumption by 28.0% and the water footprint by 41.6%, while increasing annual wheat-equivalent yield by 31.7%. These gains were achieved through optimized deficit irrigation—specifically, irrigating only when soil water content at 40 cm depth reached 60% of field capacity—which reduced deep percolation by 18.3–39.4% without any yield penalty. For Qazvin's rain-fed systems, this suggests promoting drought-tolerant crop rotations or integrating supplemental irrigation only during critical growth stages, rather than abandoning rain-fed farming altogether.

Third, for areas where rain-fed agriculture becomes increasingly marginal, integrated farming systems (IFS) offer a pathway to build resilience. In this context, policy support for Qazvin should extend beyond crop suitability mapping to include investments in water harvesting, agroforestry, and livestock integration—particularly in zones where pure rain-fed cropping is no longer viable.

Acknowledgments

This article is based on a research project titled " Moisture Stress Zoning of the Wheat Planet using SMAP Level-4 Root Zone Soil Moisture during 2015-2023 in Qazvin Province was conducted with

financial and moral support from the the Management and Planning Organization of Qazvin Province. We extend our gratitude to the the Management and Planning Organization of Qazvin.

Data Availability Statement

The climatic and topographic datasets used in this study are publicly available from the WorldClim database (https://www.worldclim.org) and EarthEnv (http://www.earthenv.org/topography). Soil data were obtained from the SoilGrids database (https://soilgrids.org/). The shapefile for rain-fed cropland in Qazvin Province was obtained from the Planning and Management Organization of Qazvin Province and is available upon reasonable request from the corresponding author.

References

1. Abolhasani, H. Khosravi, G. Zehtabian, O. Rahmati, E. Heydari Alamdarloo, P. D'Odorico, 2024. Contribution of predictive factors of land degradation occurrence applying maximum entropy model. Arid Land Res. Manag., 0 (0), pp. 1-19, 10.1080/15324982.2023.2298996
2. Akinwande, M.O., Dikko, H.G. and Samson, A. (2015) 'Variance inflation factor: as a condition for the inclusion of suppressor variable(s) in regression analysis', *Open J. of Stat.*, 5(7), pp. 754–767. https://doi.org/10.4236/ojs.2015.57075
3. Akpoti, K., Kabo-Bah, A.T., Dossou-Yovo, E.R., Groen, T.A. and Zwart, S.J. (2020) 'Mapping suitability for rice production in inland valley landscapes in Benin and Togo using environmental niche modeling', *Sci. of the Total Environ.*, 709, 136165. https://doi.org/10.1016/j.scitotenv.2019.136165
4. Alegría, A., Craig, M., Langsdorf, S., Löschke, S., Möller, V., Okem, A. and Rama, B. (eds.) (2022) *Climate change 2022: impacts, adaptation and vulnerability. Contribution of Working Group II to the Sixth Assessment Report of the Intergovernmental Panel on Climate Change*. Cambridge: Cambridge University Press, pp. 37–118. https://doi.org/10.1017/9781009325844.002
5. Ali, S., Makanda, T.A., Umair, M. and Ni, J. (2023) 'MaxEnt model strategies to studying current and future potential land suitability dynamics of wheat, soybean and rice cultivation under climatic change scenarios in East Asia', *PLOS ONE*, 18(12), e0296182. https://doi.org/10.1371/journal.pone.0296182
6. Ali, S., Umair, M., Makanda, T.A., Shi, S., Hussain, S.A. and Ni, J. (2024) 'Modeling current and future potential land distribution dynamics of wheat, rice, and maize under climate change scenarios using MaxEnt', *Land*, 13(8), 1156. https://doi.org/10.3390/land13081156

7. Azadeh Ranjbar, S. , Kholghi, M. and Abdeh Kolahchi, A. (2025). Assessment and Validation of GRACE Satellite Data with Groundwater Resources Index (GRI) at Qazvin Aquifer Plain. Iranian Journal of Soil and Water Research, 56(4), 1103-1117. doi: 10.22059/ijswr.2025.383301.669806.
8. Bennie, J., Huntley, B., Wiltshire, A., Hill, M.O. and Baxter, R. (2008) 'Slope, aspect and climate: spatially explicit and implicit models of topographic microclimate in chalk grassland', *Ecol. Model.*, 216(1), pp. 47–59. https://doi.org/10.1016/j.ecolmodel.2008.04.010
9. Braunisch, V., Coppes, J., Arlettaz, R., Suchant, R., Schmid, H. and Bollmann, K. (2013) 'Selecting from correlated climate variables: a major source of uncertainty for predicting species distributions under climate change', *Ecography*, 36(9), pp. 971–983. https://doi.org/10.1111/j.1600-0587.2013.00138.x
10. Carvalho, D., Rafael, S., Monteiro, A., Rodrigues, V., Lopes, M. and Rocha, A. (2022) 'How well have CMIP3, CMIP5 and CMIP6 future climate projections portrayed the recently observed warming', *Sci. Rep.*, 12(1), 11983. https://doi.org/10.1038/s41598-022-16264-6
11. Dobrowski, S.Z., Abatzoglou, J., Swanson, A.K., Greenberg, J.A., Mynsberge, A.R., Holden, Z.A. and Schwartz, M.K. (2013) 'The climate velocity of the contiguous United States during the 20th century', *Global Change Biol.*, 19(1), pp. 241–251. https://doi.org/10.1111/gcb.12026
12. Duan, J.Q. and Zhou, G.S. (2012) 'Climatic suitability of double rice planting regions in China', *Theor. Appl. Climatol.*, 109(1–2), pp. 129–141. DOI: 10.3864/j.issn.0578-1752.2012.02.003
13. Elith, J., Graham, C.H., Anderson, R.P., Dudík, M., Ferrier, S., Guisan, A. and Zimmermann, N.E. (2006) 'Novel methods improve prediction of species' distributions from occurrence data', *Ecography*, 29(2), pp. 129–151. https://doi.org/10.1111/j.2006.0906-7590.04596.x
14. Elith, J., Phillips, S.J., Hastie, T., Dudík, M., Chee, Y.E. and Yates, C.J. (2011) 'A statistical explanation of MaxEnt for ecologists', *Divers. Distrib.*, 17(1), pp. 43–57. https://doi.org/10.1111/j.1472-4642.2010.00725.x
15. Eyring, V., Bony, S., Meehl, G.A., Senior, C.A., Stevens, B., Stouffer, R.J. and Taylor, K.E. (2016) 'Overview of the Coupled Model Intercomparison Project Phase 6 (CMIP6) experimental design and organization', *Geosci. Model Dev.*, 9(5), pp. 1937–1958. https://doi.org/10.5194/gmd-9-1937-2016

16. FAO (2018) *The state of food and agriculture 2018: migration, agriculture and rural development*. Rome: Food and Agriculture Organization of the United Nations.
17. Feng, L., Wang, H., Ma, X., Peng, H. and Shan, J. (2021) 'Modeling the current land suitability and future dynamics of global soybean cultivation under climate change scenarios', *Field Crops Res.*, 263, 108069. https://doi.org/10.1016/j.fcr.2021.108069
18. Fick, S.E. & Hijmans, R.J. (2017). WorldClim 2: new 1-km spatial resolution climate surfaces for global land areas. International Journal of Climatology, 37(12), 4302–4315.
19. Fois, M., Cuena-Lombraña, A., Fenu, G. and Bacchetta, G. (2018) 'Using species distribution models at local scale to guide the search of poorly known species: review, methodological issues and future directions', *Ecol. Model.*, 385, pp. 124–132. https://doi.org/10.1016/j.ecolmodel.2018.07.018
20. Gao, J., Yang, X., Zheng, B., Liu, Z., Zhao, J. and Sun, S. (2020) 'Does precipitation keep pace with temperature in the marginal double-cropping area of northern China?', *Eur. J. Agron.*, 120, 126126. https://doi.org/10.1016/j.eja.2020.126126
21. Guisan, A. and Thuiller, W. (2005) 'Predicting species distribution: offering more than simple habitat models', *Ecol. Lett.*, 8(9), pp. 993–1009. https://doi.org/10.1111/j.1461-0248.2005.00792.x
22. Guisan, A. and Zimmermann, N.E. (2000) 'Predictive habitat distribution models in ecology', *Ecol. Model.*, 135(2–3), pp. 147–186. https://doi.org/10.1016/S0304-3800(00)00354-9
23. Hanley, J.A. (1989) 'Receiver operating characteristic (ROC) methodology: the state of the art', *Crit. Rev. Diagn. Imaging*, 29(3), pp. 307–335.
24. Hashemi, M., Mazandarani Zadeh, H., Zarghami, M., Demeke, B. W., Taraghi Delgarm . R., (2023). An analysis of why rehabilitation and balancing programs for aquifers do not meet water organizations' targets (a case study of the Qazvin aquifer in Iran), Agricultural Water Management, 28. https://doi.org/10.1016/j.agwat.2023.108258.
25. Hatfield, J.L. and Prueger, J.H. (2015) 'Temperature extremes: effect on plant growth and development', *Weather Clim. Extrem.*, 10, pp. 4–10. https://doi.org/10.1016/j.wace.2015.08.001
26. Hijmans, R.J., Cameron, S.E., Parra, J.L., Jones, P.G. & Jarvis, A. (2005). Very high resolution interpolated climate surfaces for global land areas. International Journal of Climatology, 25(15), 1965–1978.

27. IPCC (2014) *Climate change 2014: impacts, adaptation, and vulnerability. Contribution of Working Group II to the Fifth Assessment Report of the Intergovernmental Panel on Climate Change*. Cambridge: Cambridge University Press.
28. Javadi, A., Ghahremanzadeh, M., Sassi, M., Javanbakht, O. and Hayati, B. (2024) 'Impact of climate variables change on the yield of wheat and rice crops in Iran (application of stochastic model based on Monte Carlo simulation)', *Comput. Econ.*, 63(3), pp. 983–1000. https://doi.org/10.1007/s10614-023-10389-0
29. Ji, Y., Zhou, G., He, Q. and Wang, L. (2018) 'The effect of climate change on spring maize (Zea mays L.) suitability across China', *Sustainability*, 10(10), 3804. https://doi.org/10.3390/su10103804
30. Kochkov, D., Yuval, J., Langmore, I., Norgaard, P., Smith, J., Mooers, G. and Hoyer, S. (2024) 'Neural general circulation models for weather and climate', *Nature*, 632(8027), pp. 1060–1066. https://doi.org/10.1038/s41586-024-07744-y
31. Kogo, B. K., Kumar, L., & Koech, R. (2019). Climate change and variability in Kenya: a review of impacts on agriculture and food security. *Environment, Development and Sustainability*, 23(1), 23-43. https://doi.org/10.1007/s10668-019-00573-0
32. Kousali, M., Salarijazi, M., & Ghorbani, K. (2022). Estimation of non-stationary behavior in annual and seasonal surface freshwater volume discharged into the Gorgan Bay, Iran. Natural Resources Research, 31, 835–847.
33. Liu, Z., Yang, P., Tang, H., Wu, W., Zhang, L., Yu, Q. and Li, Z. (2015) 'Shifts in the extent and location of rice cropping areas match the climate change pattern in China during 1980–2010', *Reg. Environ. Change*, 15, pp. 919–929. https://doi.org/10.1007/s10113-014-0677-x
34. Machovina, B. and Feeley, K.J. (2013) 'Climate change driven shifts in the extent and location of areas suitable for export banana production', *Ecol. Econ.*, 95, pp. 83–95. https://doi.org/10.1016/j.ecolecon.2013.08.004
35. Mahmoodi, S., Ahmadi, K., Zahravi, M. and Karami, O. (2022) 'Modeling of Iranian oak distribution in the southwest of Iran based on the presence-based approach Maximum Entropy (MaxEnt)', *For. Res. Dev.*, 8(2), pp. 113–131. https://doi.org/10.30466/jfrd.2021.53916.1576
36. Manida, M. (2022) 'The future of food and agriculture trends and challenges', *Agric. Food E-Newsl.*, 4(2), pp. 27–29.

37. Merow, C., Smith, M.J. and Silander, J.A. (2013) 'A practical guide to MaxEnt for modeling species' distributions: what it does, and why inputs and settings matter', *Ecography*, 36(10), pp. 1058–1069. https://doi.org/10.1111/j.1600-0587.2013.07872.x
38. Moges, M.A. and Moges, S.A. (2019) 'Characteristics of future extreme precipitation and temperature in Lake Tana basin, Ethiopia', in Melesse, A.M., Abtew, W. and Senay, G. (eds.) *Extreme hydrology and climate variability*. Elsevier, pp. 59–69.
39. Mu, W., Yu, F., Li, C., Xie, Y., Tian, J., Liu, J. and Zhao, N. (2015) 'Effects of rainfall intensity and slope gradient on runoff and soil moisture content on different growing stages of spring maize', *Water*, 7(6), pp. 2990–3008. https://doi.org/10.3390/w7062990
40. Müller, C., Franke, J., Jägermeyr, J., Ruane, A.C., Elliott, J., Moyer, E. and Zabel, F. (2021) 'Exploring uncertainties in global crop yield projections in a large ensemble of crop models and CMIP5 and CMIP6 climate scenarios', *Environ. Res. Lett.*, 16(3), 034040. https://doi.org/10.1088/1748-9326/abd8fc
41. Nogueira, D.B., de Sousa, A.M., da Silva, A.O., Costa, B.R.S., da Silva Arruda, R. and Putti, F.F. (2024) 'Cropping calendar, agroclimatic and agroecological zoning for rainfed maize (Zea mays L.) under different rainfall scenarios in a semi-arid region of Brazil', *Crop Pasture Sci.*, 75(5). https://doi.org/10.1071/CP23117
42. O'Neill, B.C., Tebaldi, C., Van Vuuren, D.P., Eyring, V., Friedlingstein, P., Hurtt, G. and Sanderson, B.M. (2016) 'The scenario model intercomparison project (ScenarioMIP) for CMIP6', *Geosci. Model Dev.*, 9(9), pp. 3461–3482. https://doi.org/10.5194/gmd-9-3461-2016
43. Phillips, S.J., Anderson, R.P. and Schapire, R.E. (2006) 'Maximum entropy modeling of species geographic distributions', *Ecol. Model.*, 190(3–4), pp. 231–259. https://doi.org/10.1016/j.ecolmodel.2005.03.026
44. Portmann, F. T., Siebert, S., & Döll, P. (2010). MIRCA2000—Global monthly irrigated and rainfed crop areas around the year 2000: A new high-resolution data set for agricultural and hydrological modeling. *Global Biogeochemical Cycles*, 24(1), GB1011. https://doi.org/10.1029/2008GB003435
45. Rahimian Boogar, A., Salehi, H., Pourghasemi, H.R. and Blaschke, T. (2019) 'Predicting habitat suitability and conserving Juniperus spp. habitat using SVM and Maximum Entropy machine learning techniques', *Water*, 11(10), 2049. https://doi.org/10.3390/w11102049
46. Rockström, J. and Falkenmark, M. (2015) 'Agriculture: increase water harvesting in Africa', *Nature*, 519(7543), pp. 283–285. https://doi.org/10.1038/519283a

47. Rockström, J., Karlberg, L., Wani, S.P., Barron, J., Hatibu, N., Oweis, T. and Qiang, Z. (2010) 'Managing water in rainfed agriculture—the need for a paradigm shift', *Agric. Water Manag.*, 97(4), pp. 543–550. https://doi.org/10.1016/j.agwat.2009.09.009
48. Sadeghi, A. , Moogouei, R. , Malmasi, S. and Gharagozlou, A. (2025). Modeling Land use Changes and Providing an Optimal Model for Urban Expansion, Case Study: Qazvin City. Journal of Urban Ecology Researches, 16(41), 117-138. doi: 10.30473/grup.2024.70674.2837.
49. Shi, W., Wang, M., Tao, F., Xu, X., Deng, X., Liu, L., Kong, X., Zuo, L., Lei, M., Shi, X., & Wang, X. (2024). Wheat redistribution in Huang-Huai-Hai, China, could reduce groundwater depletion and environmental footprints without compromising production. *Communications Earth & Environment*, 5 (1), 380. https://doi.org/10.1038/s43247-024-01547-9
50. Sun, W.T. and Liu, Y.T. (2010) 'Research progress of risk analysis of biological invasion', *Chin. Agric. Sci. Bull.*, 26(7), pp. 233–236.
51. Tapas, M. R., Howard, G., Etheridge, R., Mair, M., & Peralta, A. (2025). Integrating human decision-making into a hydrological model to accurately estimate the impacts of agricultural policies. *Communications Earth & Environment*, 6, Article 412. https://doi.org/10.1038/s43247-025-02325-x
52. Tebaldi, C., Debeire, K., Eyring, V., Fischer, E., Fyfe, J., Friedlingstein, P. and Ziehn, T. (2021) 'Climate model projections from the scenario model intercomparison project (ScenarioMIP) of CMIP6', *Earth Syst. Dyn.*, 12(1), pp. 253–293. https://doi.org/10.5194/esd-12-253-2021
53. Tesfay, M. (2020) *Impacts of climate change and variability on agriculture in the Tana Beles Sub-Basins: an agro ecological based approach*. PhD thesis. Addis Ababa University.
54. Touzé-Peiffer, L., Barberousse, A. and Le Treut, H. (2020) 'The Coupled Model Intercomparison Project: history, uses, and structural effects on climate research', *Wiley Interdiscip. Rev. Clim. Change*, 11(4), e648. https://doi.org/10.1002/wcc.648
55. van Steenderen, C.J. and Sutton, G.F. (2024) 'Climate covariate selection influences MaxEnt model predictions and predictive accuracy under current and future climates', *Ecol. Model.*, 498, 110872. https://doi.org/10.1016/j.ecolmodel.2024.110872
56. Wang, X., et al. (2021). Non-stationary response of rain-fed spring wheat yield to future climate change in northern latitudes. *Science of the Total Environment*, 780, 146583.

57. Wani, S.P., Sreedevi, T.K., Rockström, J. and Ramakrishna, Y.S. (2009) 'Rainfed agriculture-past trends and future prospects', in Wani, S.P., Rockström, J. and Oweis, T. (eds.) *Rainfed agriculture: unlocking the potential*. Wallingford: CABI, pp. 1–35.
58. Yang, X. and Huang, P. (2023) 'Improvements in the relationship between tropical precipitation and sea surface temperature from CMIP5 to CMIP6', *Clim. Dyn.*, 60(11), pp. 3319–3337. https://doi.org/10.1007/s00382-022-06519-3
59. Yue, Y., Zhang, P. and Shang, Y. (2019) 'The potential global distribution and dynamics of wheat under multiple climate change scenarios', *Sci. Total Environ.*, 688, pp. 1308–1318. https://doi.org/10.1016/j.scitotenv.2019.06.143
60. Zarabian, M., Soloki, M., Boogar, A.R., Ramazan, D. and Bameri, A. (2023) 'Application of the MaxEnt model to evaluate the habitat suitability of dog rose (Rosa canina L.) in the natural landscape of Kadkan (Khorasan Razavi)', *Ecol. Inform.*, 75, 102025. http://flowerjournal.ir/article-1-246-en.html.
61. Zhang, H., et al. (2022). Copula-based drought risk analysis on rainfed agriculture under stationary and non-stationary settings. *Hydrological Sciences Journal*, 67 (11), 1683–1701.